Hindawi
Geofluids
Volume 2022, Article ID 8125317, 15 pages
https://doi.org/10.1155/2022/8125317

Research Article

Shale Heterogeneity in Western Hunan and Hubei: A Case Study from the Lower Silurian Longmaxi Formation in Well Laidi 1 in the Laifeng-Xianfeng Block, Hubei Province

Peng Zhang[1], **Junwei Yang**[1], **Yuqi Huang**[1], **Jinchuan Zhang**[2], **Xuan Tang**[2] and **Chengwei Liu**[1]

[1]*School of Mining & Civil Engineering, Liupanshui Normal University, Liupanshui 553004, China*
[2]*School of Energy, China University of Geosciences (Beijing), Beijing 100083, China*

Correspondence should be addressed to Junwei Yang; 86635174@qq.com

Received 9 October 2021; Accepted 1 December 2021; Published 7 January 2022

Academic Editor: Kouqi Liu

Shale heterogeneity directly determines the alteration ability and gas content of shale reservoirs, and its study is a core research topic in shale gas exploitation and development. In this study, the shale from the Longmaxi Formation from well Ld1 located in western Hunan and Hubei is investigated. The shale's heterogeneity is analyzed based on shale mineral rocks, microslices, geochemistry, and low-temperature N_2 adsorption-desorption. It is found that the shales of the Longmaxi Formation from well Ld1 are mainly composed of siliceous shale, mixed shale, and clayey shale. The three types of shale facies exhibit strong heterogeneity in terms of the occurrence state of organic matter, organic content, mineral composition, microstructure and structure, brittleness, and micropore type. Sedimentation, late diagenesis, and terrigenous input are the main factors influencing the shale's heterogeneity. With a total organic carbon (TOC) of 0.41%-4.18% and an organic matter maturity (R_o) of 3.09%-3.42%, the shales of the Longmaxi Formation from well Ld1 are in an overmature stage, and their mineral composition is mainly quartz (5%-66%) and clay minerals (17.8%-73.8%). The main pore types are intergranular pores, intragranular pores, microfractures, and organic pores. The results of the low-temperature N_2 adsorption-desorption experiment show that the shale pores are mainly composed of micropores and mesopores with narrow throats and complex structures, and their main morphology is of a thin-necked and wide-body ink-bottle pore. Based on the Frenkel-Halsey-Hill (FHH) model, the pore fractal dimension is studied to obtain the fractal dimension $D1$ (2.73-2.76, mean 2.74) under low relative pressure ($P/P_0 \leq 0.5$) and $D2$ (2.80-2.89, mean 2.85) under high relative pressure ($P/P_0 > 0.5$). The shales of the Longmaxi Formation in the study area have a strong adsorption and gas storage capacity; however, the pore structure is complex and the connectivity is poor, which, in turn, imposes high requirements on reservoir reformation measures during exploitation. Moreover, the fractal dimension has a positive correlation with organic matter abundance, TOC, clay mineral content, and pyrite content and a negative correlation with quartz content. Since the organic matter contained in the shales of the Longmaxi Formation in the study area is in the overmature stage, the adsorption capacity of the shales is reduced, and the controlling effect of organic matter abundance on the same is not apparent.

1. Introduction

The formation of shale reservoirs is influenced by tectonic movements, sedimentation, and late diagenesis. Both macroscopic properties (rock composition, texture/structure, spatial distribution, etc.) and microscopic properties (organic matter occurrence, pore network, mechanical parameters, etc.) are strongly heterogeneous,, and therefore, studies on heterogeneity are important ways to gain insights into reservoir characteristics [1–3]. Many domestic and international studies have shown that microscopic heterogeneity has a great influence on shale gas storage [4–7], enrichment, and migration in the following ways: (1) the mineral composition of shale reservoirs is complex, and their mineral and

organic matter compositions play an important role in the occurrence and enrichment of shale gas; (2) the heterogeneity of nanoscale pore structures and distributions of shales, and the development characteristics of fissures and microfissures result in different shale gas contents, gas release capacity, and gas seepage and affect the production of shale gas; (3) carbon and sediment are buried underground and give rise to different organic matter occurrence states through complex and diverse sedimentation and diagenesis processes [8]. Organic matter not only affects the hydrocarbon generation capacity of shale but also affects the diagenesis process and the development of organic matter pores, thus, affecting the shale reservoir's performance and its gas-bearing characteristics [9]. In addition, the occurrence state of organic matter is affected by inorganic components [10], and the composite compound degree of inorganic and organic matter usually exceeds 85%. Organic matter in shale exists in disseminated organic matter, in the mineral asphalt matrix, in organic clay complexes, organic matter-stucco complexes, etc. Studies on shale heterogeneity usually deal with macroheterogeneity and microheterogeneity up to the micron level. However, shale gas materializes in the pores of nanoscale organic matter and minerals of shale reservoirs in various forms, such as through adsorption, dissociation, and dissolution, and its reservoir space is even smaller than the micro-scale; therefore, a more detailed study on shale heterogeneity is necessary [11, 12]. The heterogeneity of shale itself has a great influence on its quality and alteration ability and plays a critical role in controlling the enrichment and high yield of shale gas in the late period. The region of western Hunan and Hubei is a key shale gas development area adjacent to the Sichuan Basin. Previous studies in this region have mostly focused on the content characteristics and vertical and horizontal changes in organic matter. However, there have been few studies on different shale mineral compositions/lithofacies characteristics, micro-nanoscale organic matter occurrence, micropore and pore structures, rock mechanical properties, etc. [13–15]. In this study, the marine shale of the Longmaxi Formation in Laifeng, Hubei is taken as the research object, and the lithofacies in this Formation are analyzed and categorized. The genesis and morphology of inorganic minerals and their contact relationship with organic matter are analyzed at the micro-nanoscale, and the occurrence modes of inorganic minerals and organic matter in different shale lithofacies are established. A comparative study on the differences in the total organic carbon, pore types, pore characteristics, and pore size distribution in different lithofacies is carried out to reveal the diverse development mechanisms of the shale reservoir. In addition, the heterogeneity characteristics of the pore structure of the marine shale reservoirs are studied to quantify the heterogeneity parameters of the pore structure and discuss their influence on the occurrence and migration of shale gas.

2. Geological Background

The study area is located in the central part of the Yangtze paraplatform and southwest wing of the Yidu-Hefeng anticline in the Western Hunan Hubei fold-thrust belt in the middle of the Yangtze paraplatform, and a small part is located in the Huaguoping anticline. The entire area trends NE-SW, and the Lianghekou syncline is relatively wide and gentle. Under the influence of the early Caledonian movement, the area of the Yangtze plate in the late Ordovician increased and gradually extended to the Yangtze region, making the Yangtze sea occur in a semiclosed state. The crust in the middle and upper Yangtze region sank and the sea level rose, depositing a set of siliceous shale, which is one of the main source rocks in the region. The Indosinian movement ended the marine sedimentary history of the middle upper Yangtze paraplatform and formed the rudiment of the present structure in the study area [16]. The early Yanshanian fold movement had the greatest impact on the study area, resulting in the strong deformation of the entire area's caprock and the formation of NE trending folds and faults, which basically established the current structural pattern. This period was also the main hydrocarbon generation period of the Longmaxi Formation. From the late Yanshanian to the early Himalayan, the middle and upper Yangtze region entered a stage of extensional action of great significance in the Pacific tectonic domain. However, the activities of this stage are different from east to west and from north to south. Western Hunan and Hubei were less affected by the late Yanshanian early Himalayan tectonic movement, and the tectonic features formed in the early Yanshanian are basically unchanged. In the late Himalayan period, the study area suffered strong uplift and denudation, resulting in the upper Paleozoic and Mesozoic strata remaining only in the syncline core, while the lower Paleozoic strata in the anticline core are exposed at the surface (Figure 1).

3. Experiment and Methods

3.1. Samples and Logging Response Characteristics. The shale samples used in the experiment were taken from the core of the Longmaxi Formation in well Ld1. The well was drilled 20 m into the Upper Ordovician Pagoda Formation, and the target stratum was the lithologic member enriched with organic matter of the Longmaxi Formation in the Silurian system, with a depth of 898.16~949.10 m and a thickness of 50.94 m. Based on the characteristics of the sudden change in the lithology and lithofacies, rapid deepening or shallowing of the water depth and obvious changes in the logging curve shape, the Longmaxi formation is divided into three members from bottom to top, namely, the Long 1 member (929.41~949.10 m), the Long 2 member (910.31~929.41 m), and the Long 3 member (898.16~910.31 m). The two interfaces of the Long 2 member, the Long 1 member, and the Long 3 member show lithologic mutation, and the response characteristics of the logging curves are also similar. Lithologically, the two interfaces change from argillaceous siltstone below to carbonaceous silty shale above. In the logging curves, the GR curve changes suddenly from bottom to top, the GR value above the interface increases obviously, the curve shape changes from straight sawtooth to bell, the AC curve is a sudden interface, the AC value above the bottom interface increases obviously, and the RD

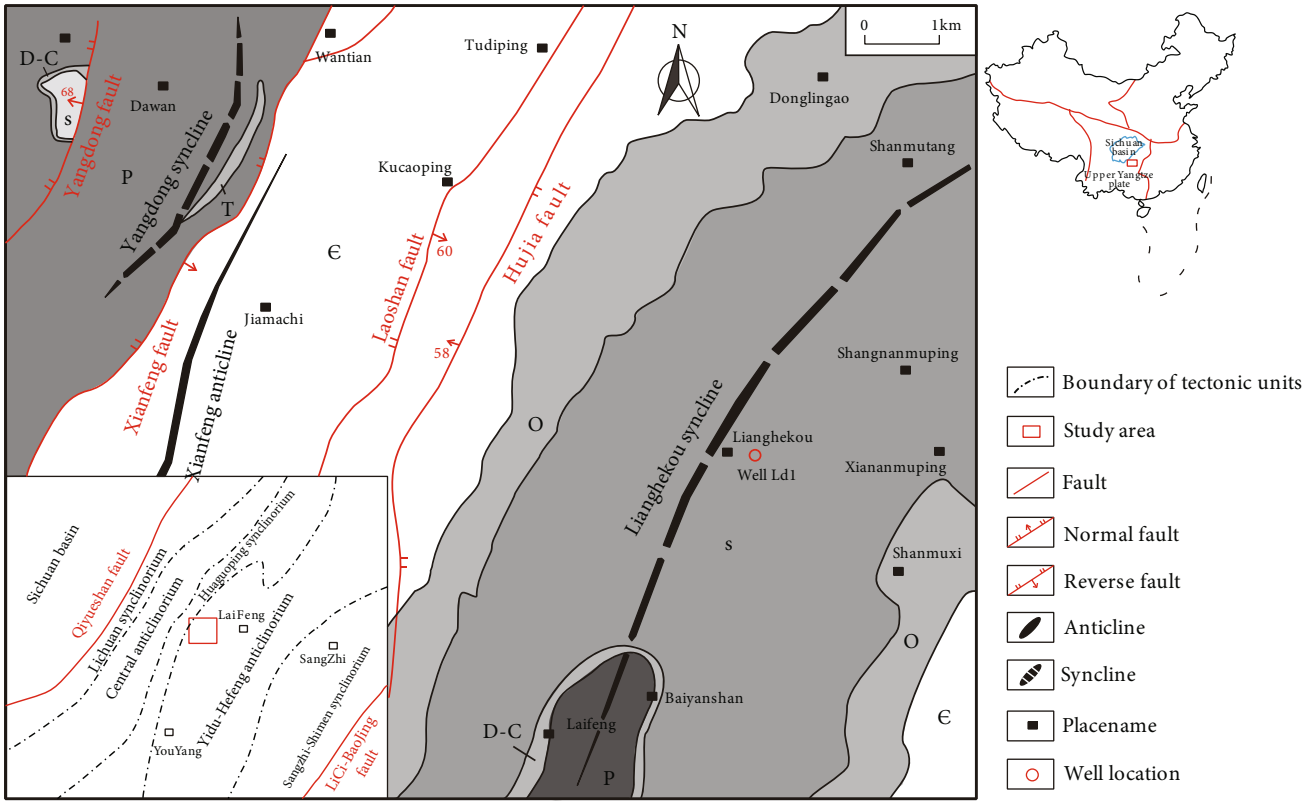

Figure 1: Geological background and location of well Ld1 in the study area.

value decreases [17]. The sedimentary environment fluctuates from deep-water shelf facies in the lower part of the Longyi member to shallow water shelf facies and tidal flat facies above (Figure 2).

3.2. Experiment Instruments and Methods. The X-ray diffraction (XRD) experiment was conducted with a D8 ADVANCE X-ray diffractometer (Bruker, Germany) under the conditions of Cu target, Kα radiation, X-ray tube, a voltage of 40 kV, and an electric current of 30 mA. A comparative analysis was carried out based on the standard powder diffraction data provided by the International Centre for Diffraction Data (ICDD) and according to its standard analysis methods and diffraction criteria (consistent interplanar spacing and diffraction intensity). About 50-100 g of samples was taken at each sampling site, and they were crushed and divided into samples of about 5 g. The collected samples were ground in a grinding bowl to a particle size of 48 pm.

The TOC experiment was conducted with a C-S580A carbon-sulfur analyzer (Germany). According to the national standard SYT-T5116-1997, the samples were processed with dilute hydrochloric acid to remove the carbonate. According to the repeated analysis of the standard samples, the TOC analysis accuracy was greater than 0.5%. The vitrinite reflectance (Ro) was measured with a microphotometer at a temperature of 23°C and a humidity of 30%. The microscope was amplified 125 times, with a resolution of 0.01%.

The microsurface morphology and structural characteristics of the shale samples were observed under a ZEISS SIGMA field emission scanning electron microscope. When the shale samples were prepared, their surface was etched using Ar-ion milling technology and bombarded by a high-speed ion beam to form an ultrasmooth surface that cannot be obtained through conventional mechanical milling; this was done to avoid damage to the surface of the shale samples caused by mechanical milling and to retain the original pore morphology on the surface. Afterward, gold film with a thickness of 10-20 nm was plated on the milled surface to enhance its conductivity.

A micromeritics ASAP 2020 specific surface area and porosity adsorption instrument (America) was used to carry out the low-temperature nitrogen adsorption experiment on the samples. Its measuring aperture range is 0.35-500 nm, and the lower limit of the specific surface was 0.0005 m^2/g. Before the experiment, the samples were first vacuumed at a high temperature of approximately 150°C to remove the remaining bound water and capillary water. Then, nitrogen, with a purity above 99.999%, was taken as the absorbate to measure the adsorption capacity of the samples under different relative pressures. Next, the nitrogen adsorption-desorption isothermal curve was recorded and plotted with the relative pressure as the abscissa and the adsorption capacity of the unit mass sample as the ordinate. According to the BET equation, the BET linear graph was plotted with a relative pressure range of 0.05-0.35; the specific surface area of the shale sample was obtained, and the desorption branch of the nitrogen adsorption isothermal curve was calculated using the Barret-Joyner-Halenda aperture distribution test

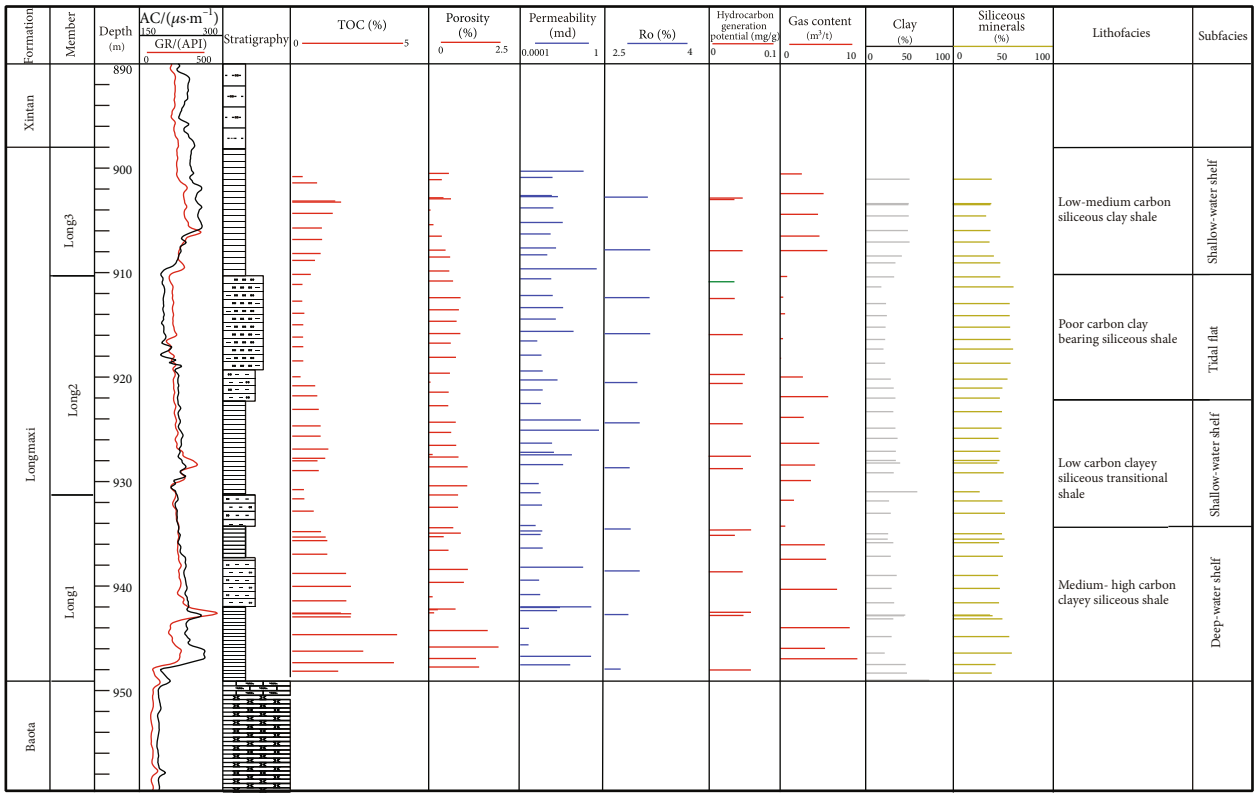

Figure 2: Comprehensive column of the Longmaxi Formation in well Laidi 1 in the Laifeng-Xianfeng block, Hubei Province.

(BJH) method to obtain the pore size distribution of the shale sample.

4. Rock Matrix Heterogeneity

Shale is mainly composed of inorganic minerals, organic matter, and pores. Inorganic minerals and organic matter constitute the rock matrix. The properties of the rock matrix have an important impact on the development of the reservoir space and its gas storage performance. Therefore, studying the properties of the rock matrix is of great significance in the study of reservoir properties. Specifically, organic matter and clay minerals are the main factors that determine the adsorption capacity of shale, and a high content of brittle minerals is a key factor affecting the cost and efficiency of shale gas exploitation in the late stage. The nanoscale pores in shale are the main space where free shale gas resides. Therefore, studies on the heterogeneity of shale matrixes and organic matter are of great significance to identify and exploit high-quality gas-bearing intervals. Shale lithofacies is the external representation of various heterogeneity characteristics of shale enriched with organic matter and includes macro in formation, such as rock type, structure, and construction, and microinformation, such as inorganic minerals and organic composition; it is a direct evaluation indicator of the original shale quality [18–20].

4.1. Shale Minerals and Organic Geochemical Characteristics. X-ray diffraction tests on 54 shale samples from well Ld1 show that the shale is mainly composed of quartz (5%-66%, mean 36.9%) and clay minerals (17.8%-73.8%, mean 39.4%), followed by feldspar (3.2%-25.4%, mean 14.7%), carbonate minerals (0.6%-13.7%, mean 5.5%), and pyrite (0.7%-9.6%, mean 2.8%). Among them, the clay minerals include illite (39%-81%, mean 58%), illite/smectite (4%-58%, mean 29%), and chlorite (4%-21%, mean 12.5%). The main organic matter type is type II_1, followed by type II_2; the macerals are mainly represented by saprolite and inertinite and lack vitrinite and exinite; the saprolite is dominated by disseminated mineral asphalt matrixes. According to the analysis of 45 samples, the TOC of the shale is 0.33% ~ 4.18% and is greater than 1% in the main body, with an average of 1.33%. Specifically, the TOC of Member 1, Member 2, and Member 3 is 0.48% ~4.18% (mean: 2.05%), 0.33% ~1.44% (mean: 0.77%), and 0.42% ~1.95% (mean: 1.24%), respectively. The organic matter maturity (R_o) of 11 samples ranges from 2.79% to 3.32%, with an average of 3.11%. The samples are in the overmature stage, and their overall maturity increases from bottom to top [21–23]. This can be attributed to the organic matter in the upper part of the Longmaxi Formation being catalyzed by inorganic minerals, such as clay minerals, which promote the evolution of organic matter. Based on the data of the three members, as well as the contents of siliceous minerals (quartz + feldspar), carbonate minerals (dolomite + calcite), and clay minerals, the shale of the Longmaxi Formation can be divided into siliceous shale, clayey shale, and mixed shale, no calcareous shale is present (Figure 3), and it is divided according to the single mineral content is subdivided (10%, 25%, 50%, and 75%). By referring to the practical experience of shale

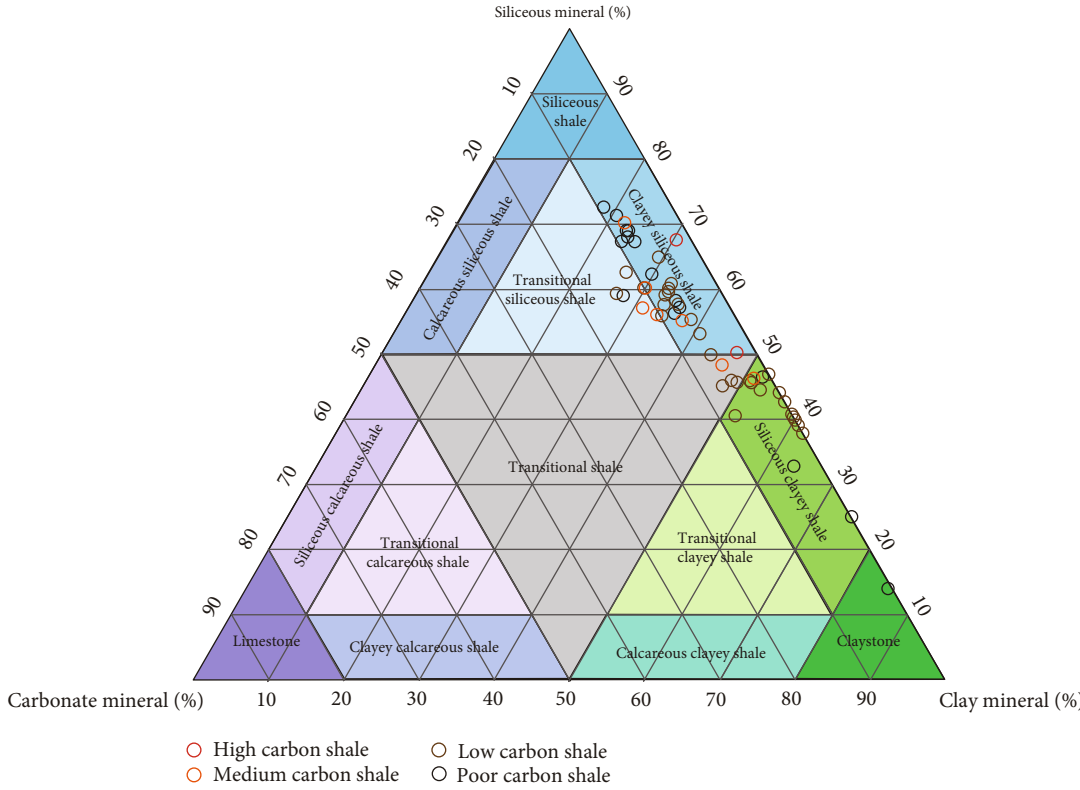

Figure 3: Classification of shale facies and comparison of organic carbon contents.

gas exploitation and development in the Sichuan Basin, the shale is divided into five types based on organic content, i.e., carbon-rich (TOC > 4%), high-carbon (3% < TOC < 4%), medium-carbon (2% < TOC < 3%), low-carbon (1% < TOC < 2%), and carbon-poor (TOC < 1%) shale, and the shale of the Longmaxi Formation can be further divided into four subgroups: medium-high carbon clayey siliceous shale, low-carbon clayey siliceous mixed shale, carbon-poor clayey siliceous shale, and low-medium carbon clayey shale.

4.2. Shale Lithofacies Characteristics

(1) Medium-high carbon clayey siliceous shale

This type of shale is mainly distributed in the lower part of Member 1, with a TOC greater than 2%. Its sedimentary environment is a deep-water continental shelf, where the rock color is deep dark and the organic content is high. The genesis and morphology of the inorganic components are diverse. Graptolites are developed in great quantity and dominated by orthograptus in hypertrophic shapes, where a large number of radiolarians can be observed. The quartz mainly includes biological quartz, diagenetic authigenic quartz, and a small amount of terrigenous quartz, with a high content of quartz and an average value of greater than 50%; the content of clay minerals is low, ranging from 25% to 36%; the content of carbonates is lower than 10%; pyrite is relatively developed, and includes framboidal pyrite, pyrite aggregate, etc. Microcrystalline quartz, clay minerals, and pyrite are encapsulated in contiguous solid asphalt, and framboidal pyrite is also rich in organic matter; in the longitudinal direction, the heterogeneity of organic matter occurrence in this lithofacies is weak, and the cyclical change in the sedimentary environment is not obvious (Figure 4(a)).

(2) Low-carbon clayey siliceous mixed shale

This type of shale has a TOC lower than the medium-high carbon clayey siliceous shale, and its organic carbon content, which is mainly distributed in Member 2, is 1%-2%. The sedimentary environment is a shallow-water continental shelf, and the inorganic components are also diverse, but their proportion varies with different genesis. The content of quartz is 40%~50%, and the amount of terrigenous quartz is greatergreathigh, with large particle sizes and subangular edges; the content of clay minerals is 40%~50%, and a small amount of carbonate and pyrite is present. The content of graptolite is high, and solid asphalt exists between the terrigenous quartz particles and clay minerals. Because the content of terrigenous quartz and clay minerals is higherhigh and the organic content is lowerlow, this shale has little difference from clay siliceous shale (Figure 4(b)).

(3) Carbon-poor clayey siliceous shale

Compared with the low-carbon clayey siliceous mixed shale, this shale has a lower TOC (less than 1%). It is mainly distributed in the upper part of Member 1 and Member 2. The sedimentary environment is the shallow area of a

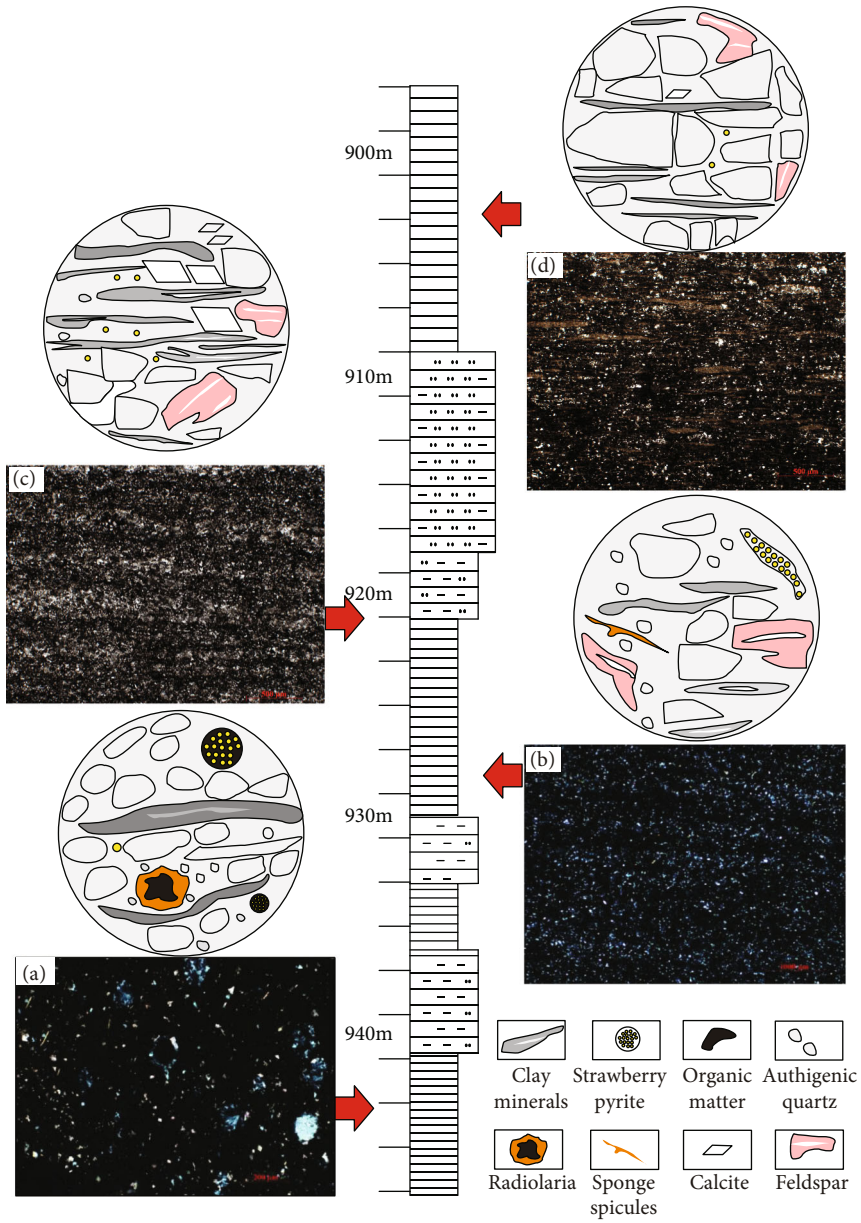

Figure 4: Lithofacies characteristics of the Longmaxi Formation in well Ld1.

shallow-water continental shelf or the lower part of the intertidal zone to the subtidal zone, with strong hydrodynamic force. The rocks have a lighter color, lower organic content, and less graptolite. Tidal bedding is developed and the inorganic components are more diverse. The content of quartz and clay minerals is lowerlow, with both ranging from 25% to 50%; the content of carbonate is higherhigh, ranging from 10% to 25%. Solid asphalt is present between the terrigenous quartz particles and the clay minerals, and there are no solid particles between the flaky laminated clay minerals that adsorb amorphous organic matter; with the reduction in the clay minerals, the adsorbed organic matter also decreases. The content of pyrite is lowerlow, so its encapsulated organic matter is also reduced. In this shale, the area of the change in the organic matter enriched with inorganic minerals (e.g., from high to low) is obvious, resulting in the frequent alternation of bright and dark laminas and clearer boundaries between laminas. The thickness of a single lamina ranges from 0.5 mm to 2.0 mm.

(4) Low-medium carbon clayey shale

This type of shale has a TOC of 1%-2% and is mainly distributed in Member 1. The sedimentary environment is a shallow-water continental shelf, and the genesis and category of inorganic components are relatively simple. Quartz is mainly terrigenous, with a large particle size and angular edges; it is poorly rounded and has a content of 30%-40%. The enrichment of organic matter is inhibited and diluted, the content of terrigenous feldspar is higherhigh, and the content of clay minerals is 50%-70%; the content of carbonate is usually not greater than 10%; pyrite is rare and is

present sporadically. Solid asphalt seldom exists between the mineral particles, and bright and dark lamina composed of framboidal pyrite and organic matter is more obvious, with the thickness of a single lamina being 0.3-3.0 mm. The organic matter is relatively enriched in the clayey lamina at the bottom, and the silty lamina at the upper part is reduced, showing a frequent alternation in the enrichment and reduction of organic matter. This feature reflects the frequent alternation of the sedimentary environment, and the geological cycle of the emergence, death, and burial of hydrocarbon-generating organisms (Figure 4(d)).

The formation of shale is controlled by various factors, such as basin structure, physical and chemical conditions of a water body, climate change, sediment supply, and regional sea-level change. The shale of the Longmaxi Formation in the study area gradually evolved in sequence from siliceous shale to mixed shale and then clayey shale. In addition, terrigenous detrital minerals and clay minerals gradually increase from the bottom to the top, with organic carbon content gradually decreasing from the bottom to the top. The shale structure gradually changes from a uniform block structure to a sandy band structure, presenting a graded bedding development. This indicates that the terrigenous detrital supply was enhanced and that the sedimentary environment transitioned from a reducing environment to an oxidizing one.

Shale brittleness evaluation is the main basis for engineering fracturing modification and interval optimization. At present, the commonly used methods include the mineral composition method, the elastic parameter method, and a combination of both. Limited by experiments and materials, the mineral composition method (w, mineral mass percent) is selected in this study to analyze shale brittleness [24], i.e.,

$$\text{Brit} = \frac{\omega_{\text{Quartz}} + \omega_{\text{Carbonate}}}{\omega_{\text{Quartz}} + \omega_{\text{Carbonate}}\omega_{\text{Clay}}}. \quad (1)$$

Through calculation, it is found that the shale brittleness of the Longmaxi Formation is 0.36-0.81, among which the brittleness of the siliceous shale is 0.59-0.81, which is significantly better than that of the clayey shale (0.35-0.48) and the mixed shale (0.49-0.53). The longitudinal changes in the brittle minerals and organic carbon content are the main causes for the heterogeneity of the shale's brittleness.

5. Reservoir Space Heterogeneity

From SEM, the development status of different pores and fractures in shale can be obtained and their parameters can be obtained semiquantitatively. According to the classification scheme of pore morphology occurrence, the pores obtained by SEM are divided into four types: organic pore, intragranular pore, intergranular pore, and micro-fissure. The pore structure of shale, i.e., pore size, distribution, throat geometry, and connectivity, controls the dynamic process of adsorption-desorption of gas molecules in shale, which is the key factor for evaluating the gas storage capacity, seepage capacity, and later development value of shale [28–31].

5.1. Pore Type Heterogeneity. The shale of the Longmaxi Formation in well Ld1 mainly contains inorganic pores (intergranular pores, flocculent mineral intragranular pores, and microfractures) and organic matter micropores. The morphology of the inorganic pores is mainly affected by the shape, contact relationship, and arrangement of particles. The development of pores in different lithofacies is highly heterogeneous. The siliceous shale was deposited in an anoxic deepwater environment, where the pyrite was relatively developed and the intergranular pores of the framboidal pyrite aggregate were almost filled with migrating organic matter. Due to the high content of authigenic quartz and detrital quartz transformed by microorganisms in the siliceous shale, more intergranular pores and intragranular pores associated with quartz particles are developed (Figure 4(c)). In addition, the shale of the Longmaxi Formation is characterized by great burial depth and a high degree of thermal evolution, and more bubble-shaped and spongy organic pores easily formed after the light hydrocarbon components generated from organic matter were released. Spongy organic pores are more commonly found in the migrating organic matter from the overmature siliceous shale (Figures 5(a)–5(c)). In the mixed shale, the content of calcite and dolomite is generally over 10%. Therefore, compared with clayey and siliceous shale, the marginal dissolution pores and intergranular dissolution pores of calcite and dolomite in the mixed shale are developed with a larger pore size (>1 μm), which is greater than the organic pores (< 150 nm) and the clayey intergranular pores (<500 nm) (Figures 4(d)–4(f)); in addition, most of the dissolution pores are filled with migrating organic matter [25, 26]. In the clayey shale, the content of clay minerals reaches up to 73.8%, while the organic content is low, and the pores are mostly interlayer pores and intergranular pores of stripped clay minerals, as well as migrating organic pores (Figures 5(g)–5(i)).

The nitrogen adsorption-desorption isothermal curve of the shale samples is shaped like a reverse "S." The adsorption isothermal curve of the shale samples belongs to the typical type IV. The desorption curve is much steeper than the adsorption curve at the medium relative pressure ($0.4 < P/P_0 < 0.6$) and shows a steep drop trend, forming a broad H2-H3 hysteresis loop (Figure 6). The adsorption and desorption curves draw closer at the end. This indicates that most of the pores are micropores and that the pore type is dominated by silty thin-necked and wide-body ink-bottle composite pores. Since the high-pressure mercury intrusion method to measure pore structures can cause shale fractures, it is difficult to distinguish microfractures produced from natural fractures. Therefore, six samples of the Longmaxi Formation in well Ld1 were analyzed using the liquid nitrogen adsorption-desorption method. The experimental results show that:the BET specific surface area of the shale of the Longmaxi Formation ranges from 5.35 m^2/g to 15.20 m^2/g, with an average of 7.90 m^2/g, which is a significant variation; the range of the average pore size is 3.48 nm~5.14 nm, with an average of 4.10 nm. According to the classification standard of the International Union of Pure and Applied Chemistry (IUPAC), pores with a pore size of

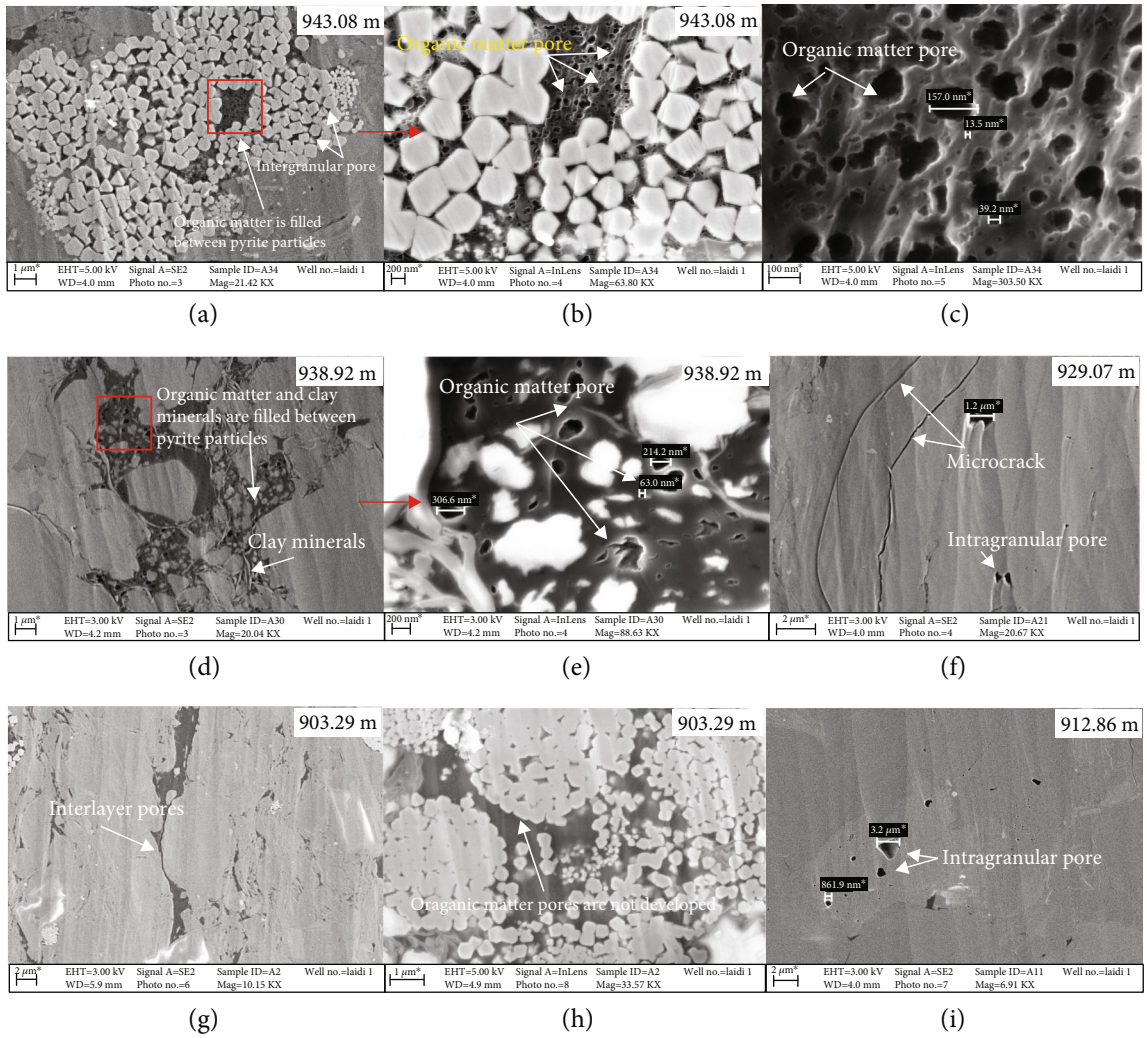

Figure 5: Pore distribution and morphological characteristics of shale.

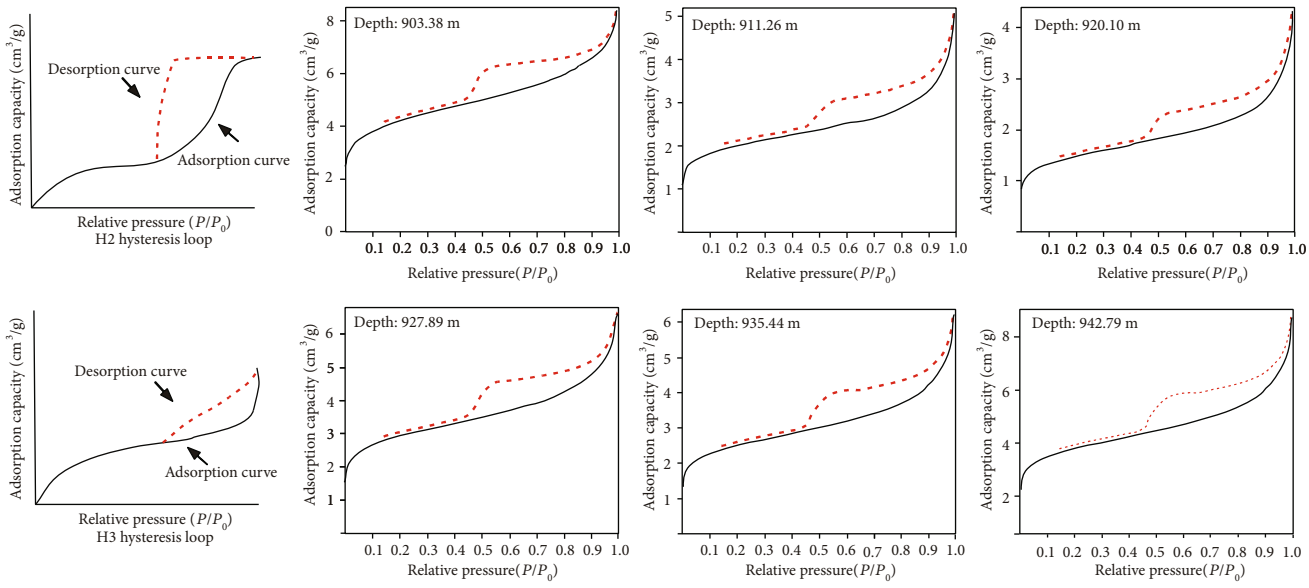

Figure 6: Characteristics of the N_2 adsorption and desorption at low temperatures in the Longmaxi Formation.

Table 1: Statistical table of the shale pore volume of the Longmaxi Formation of well Ld1.

Serial Number	Depth (m)	Pore volume (10^{-3} cm^3/g)				Pore volume ratio (%)		
		Micropore	Mesopore	Macropore	Total pore volume	Micropore	Mesopore	Macropore
1	903.38	1.93	2.87	0.14	4.94	39.1	58.1	2.8
2	911.26	0.81	1.37	0.35	2.53	32.0	54.2	13.8
3	920.10	0.57	1.05	0.31	1.93	29.5	54.4	16.1
4	927.89	1.27	2.04	0.18	3.49	36.4	58.5	5.2
5	935.44	0.99	1.38	0.13	2.50	39.6	55.2	5.2
6	942.79	1.73	2.56	0.13	4.42	39.1	57.9	2.9
Average value		1.22	1.88	0.21	3.30	36.0	56.4	7.7

less than 2 nm are micropores, those with a pore size of 2 nm-50 nm are mesopores, and those with a pore size greater than 50 nm are macropores. The samples from well Ld1 contain all these three types of pores, with micropores and mesopores forming the majority; they have the highest proportion in terms of specific surface area and pore volume. Specifically, the pore volume proportion of the micropores is 29.5% ~ 39.6% and 36.0% on average; that of the mesopores is 54.2% ~58.5%, and 56.4% on average; and that of the macropores is 2.8% ~16.1%, and 7.7% on average. It is speculated that the micropores and mesopores are the main places where shale gas is present in the Longmaxi Formation. Specifically, the intragranular pores among the pyrite and clay minerals, the organic pores, and the nanoscale microfractures are the main spaces where the shale gas is present (Table 1).

5.2. Pore Structure Heterogeneity. The fractal theory has been adopted to describe the complexity of pore structures or the surface roughness of porous media. The commonly used parameter is the fractal dimension D, which is directly proportional to the complexity of the pore structure and the surface roughness of porous media. Generally, its value is 2-3. Based on the data from the low-pressure nitrogen adsorption experiment, the calculation formula for the fractal dimension was obtained according to the Frenkel-Halsey-Hill (FHH) model [17–20]:

$$\ln V = k \ln (\ln P_0/P) + C, \quad (2)$$

$$D = k + 3, \quad (3)$$

where V is the volume of gas absorbed when the equilibrium pressure is P, in m^3; P_0 is the saturated vapor pressure, in MPa; k is a constant related to the adsorption mechanism and the fractal dimension; and C is a constant. Due to the difference in the adsorption mechanism and the pore size, there are two different pore fractal dimensions, $D1$ and $D2$, on the nitrogen adsorption curve under the relative pressure of 0-0.5 and 0.5-1, which are used to describe the surface roughness and the complexity of the pore structure of the shale pores, respectively. Also, they can be used to describe the characteristics of large and small pores in the shale (the pore size corresponding to the relative pressure of 0.5 on the nitrogen adsorption curve is the breaking point). According to equation (2), the data of the low-pressure nitrogen adsorption were organized, and ln V was plotted for ln (ln P_0/P). The slope of the different curves obtained by fitting is the value of k. Then, the fractal dimension, D, can be obtained according to equation (3).

The emergence and rapid development of fractal theories provide theoretical support for the quantitative analysis of the pore structures of shales. According to the low-temperature nitrogen adsorption experiment, the calculation models of the shale fractal dimension mainly include FHH, BET, and thermodynamic models. The FHH model is widely used in shale reservoirs and has the best fitting performance [27]. With the FHH model as the theoretical basis, mathematical calculation and piecewise fitting were carried out on the data of the low-temperature adsorption-desorption experiment (Figure 7). The fractal dimension is denoted by $D1$ in the stage with low pressure ($P/P_0 \leq 0.5$) and $D2$ in the stage with high pressure ($P/P_0 > 0.5$) in the adsorption process. According to the calculation results of the clayey shale samples of the Longmaxi Formation, $D1$ is 2.7284-2.7562 (mean 2.7432) and $D2$ is 2.7984-2.8850 (mean 2.8455) (Table 2).

5.3. Porosity and Permeability Characteristics. The porosity distribution range of 44 shale samples from the Longmaxi Formation in well Ld1 as measured by the pulse method is 0.06%-2.09%, with an average of 0.73%; among these, the porosity between 0.5% and 1% dominates, indicating that the overall porosity is relatively low. Member 1 has the highest porosity, followed by Member 2. Member 3 has the lowest porosity due to its low brittle mineral content, high clay mineral content, and weak compressive strength, as well as large pores and fissures that are filled by clay minerals. Moreover, the relative content of clay minerals and brittle minerals is an important factor that influences the porosity and permeability of shale. Through the analysis of the relationship between porosity and permeability, it has been demonstrated that the porosity and permeability of siliceous shales are significantly higher than those of other shales. Under stress, highly brittle shales are more likely to produce interconnected pore networks and fracturing-induced cracks later. The permeability range of the shales is $(0.00025 \sim 0.60) \times 10^{-3}$ μm^2, with an average of 0.0462×10^{-3} μm^2; the

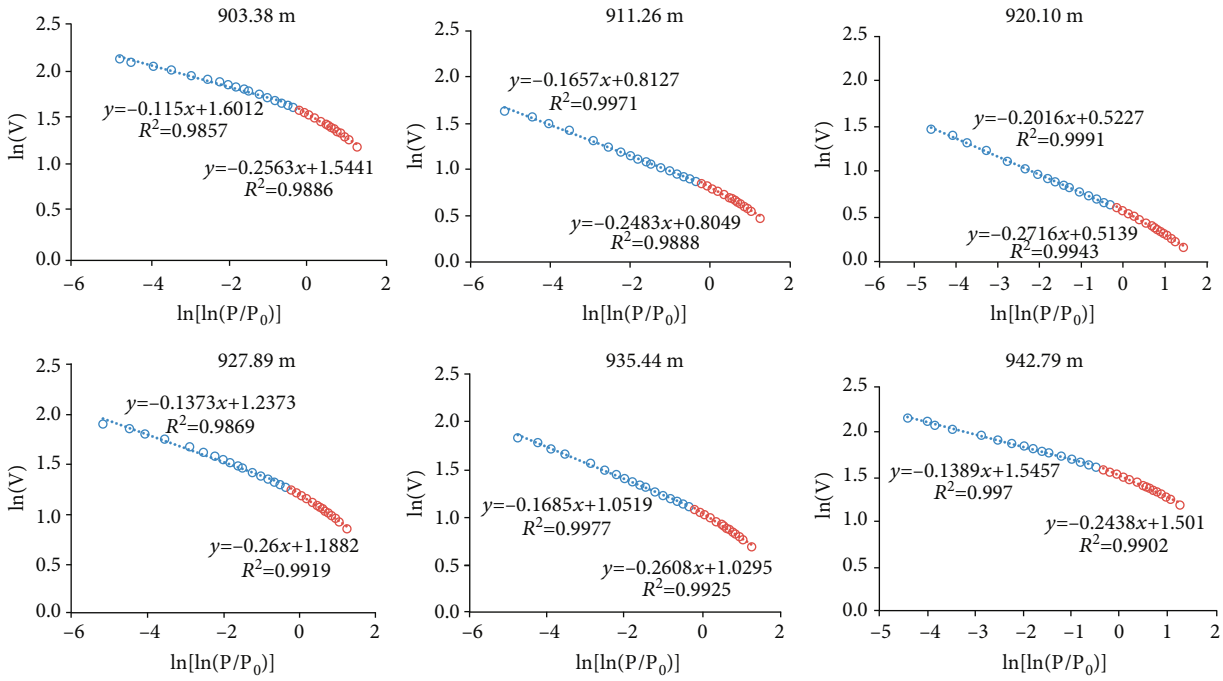

Figure 7: Fitting lines of pore fractal dimensions for the Longmaxi Formation shales.

Table 2: Fractal dimensions of the Longmaxi Formation shale from nitrogen adsorption and reservoir characteristic parameters.

Serial number	Depth (m)	$D1$	Fitting equation	$R^2/D1$	$D2$	Fitting equation	$R^2/D2$
1	903.38	2.74	$y = -0.26x + 1.54$	0.99	2.89	$y = -0.12x + 1.60$	0.99
2	911.26	2.75	$y = -0.25x + 0.8$	0.99	2.83	$y = -0.17x + 0.81$	0.99
3	920.10	2.73	$y = -0.25x + 0.8$	0.99	2.80	$y = -0.27x + 0.51$	0.99
4	927.89	2.74	$y = -0.14x + 1.24$	0.99	2.86	$y = -0.26x + 1.19$	0.99
5	935.44	2.74	$y = -0.17x + 1.05$	0.99	2.83	$y = -0.26x + 1.03$	0.99
6	942.79	2.76	$y = -0.14x + 1.55$	0.99	2.86	$y = -0.24x + 1.50$	0.99

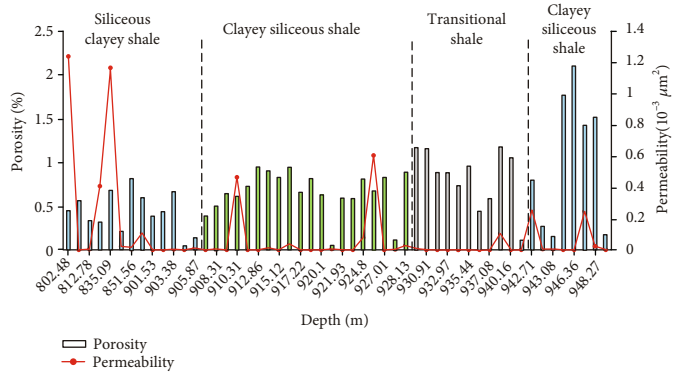

Figure 8: Pore and seepage characteristics of the Longmaxi Formation shale.

majority of the permeability lies between $(0.001 \sim 0.01) \times 10^{-3}\ \mu m^2$, with a wide range of changes. The permeability of the shales is extremely low on the whole, and the correlation between porosity and permeability is poor, which may be caused by unlinked pores (Figure 8).

6. Discussion

6.1. Effective Characterization and Evaluation of the Pore Structure. In this study, the pore structure of shale samples from the Longmaxi Formation was studied using high-

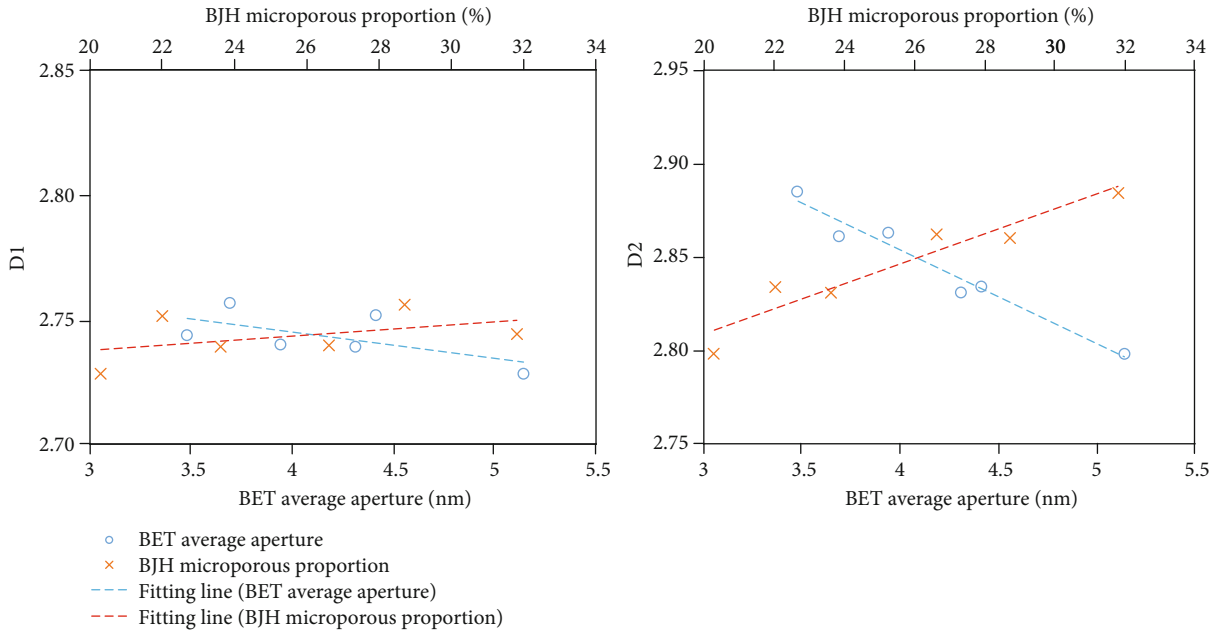

Figure 9: Relationship between fractal dimension and pore size.

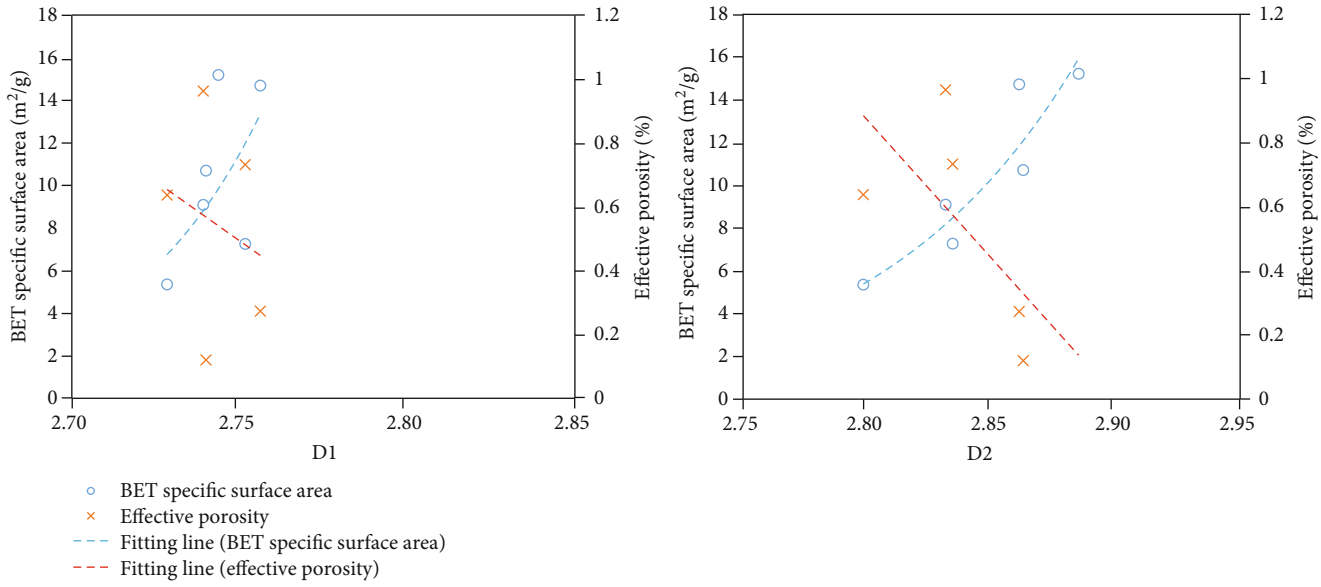

Figure 10: Relationship between reservoir property and fractal dimension.

pressure mercury intrusion and low-temperature nitrogen adsorption-desorption experiments to mainly characterize the pore size, pore complexity, etc. Comparing the correlation between the characterization parameters of different pore structures and the fractal dimension shows that the fractal dimension not only characterizes the surface roughness and complexity of the pores but also has a good correlation with the pore size (Figure 9). The smaller the average pore size in the shale, the larger is the proportion of micropores; further, the more complex the pore structure, the larger is the corresponding fractal dimension. $D2$ can better characterize the pore complexity and has a better correlation with the pore size. In contrast, although $D1$ has a certain correlation with the pore size, the complete correlation is not obvious. This is because pore size can affect shale reservoir capacity to a certain extent; however, it is not a controlling factor. $D1$ mainly reflects the rock reservoir performance, and therefore, the trend of $D1$ changing with pore size is not obvious.

Correlation analysis between the physical parameters of the shale reservoir and the fractal dimension was carried out (Figure 10), and the results show that a certain correlation exists between the effective porosity and the specific surface area of rocks and the fractal dimension. Additionally, there is a negative correlation between the effective porosity and the fractal dimension. This is because as the pore

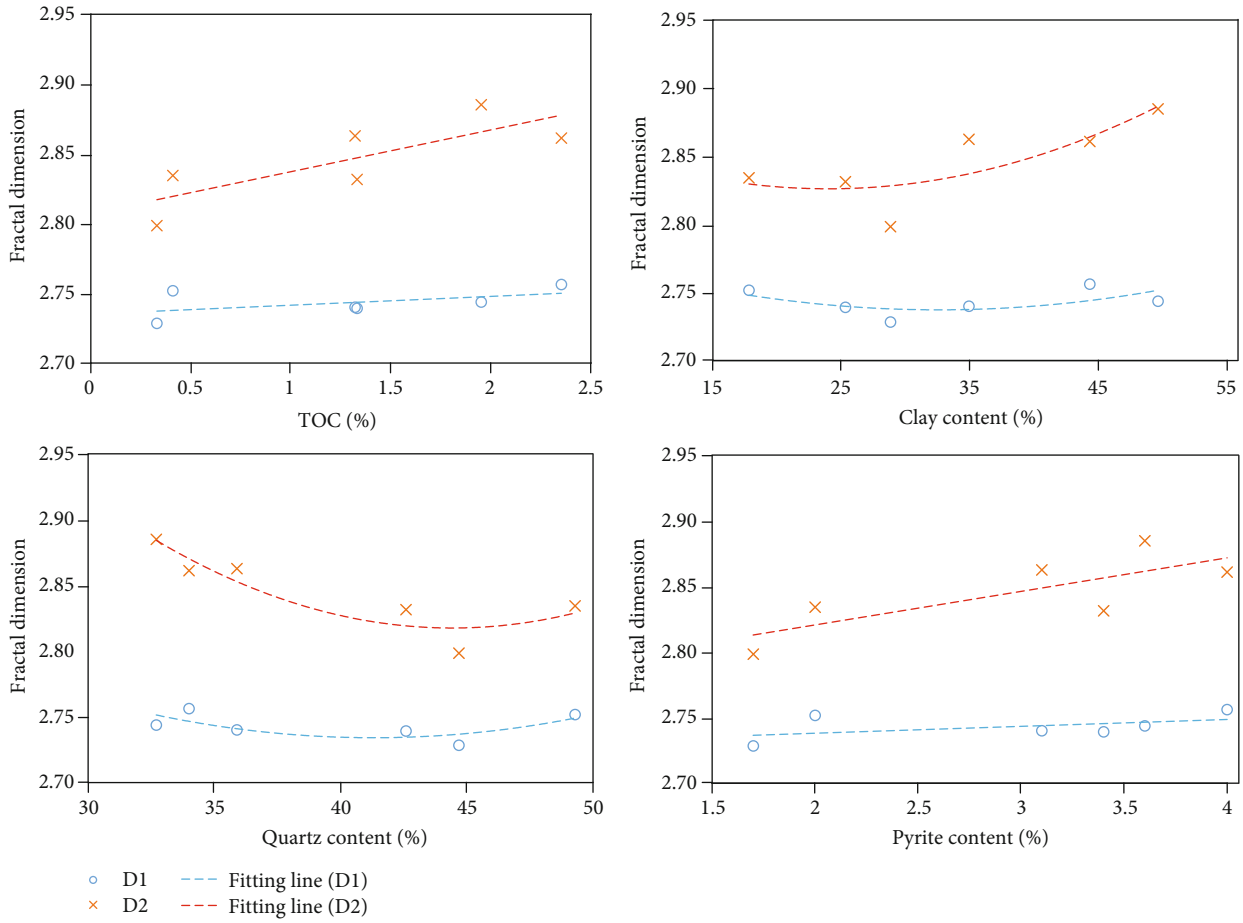

Figure 11: Main controlling factors of pore structure.

complexity increases, the connectivity of pores decreases, and a large number of independent pores that are not effective pores are formed, resulting in a decrease in the effective porosity. Although the connectivity of independent pores is poor, reflecting the unsatisfactory physical characteristics of the reservoir, they can still store fluids and are of great significance with respect to the enrichment of shale gas. In the late development stage, artificial methods are adopted to increase the pore connectivity, thereby effectively improving the reservoir's physical properties and making the gas therein recoverable. Moreover, there is a good positive correlation between the specific surface area of the shale and the fractal dimension, and the increasing trend is extremely obvious with the increase in $D1$, and the slope of the fitting curve is large. Shale gas mainly exists in shale pores in free and adsorbed states. The gas adsorption capacity of shale is an important parameter of its gas storage capacity. A greater specific surface area means a stronger adsorption capacity of shale, i.e., a larger fractal dimension. In particular, shales with a larger $D1$ have a stronger adsorption capacity.

The fractal dimension based on the low-temperature N_2 adsorption-desorption experiment is a parameter that can fully characterize the pore structure. $D1$ can effectively reflect the adsorption and gas storage capacity of shale, and $D2$ can comprehensively reflect the size and complexity of shale pores. For shale gas reservoirs, a greater $D1$ value indicates that the rocks have a stronger ability to store free gas and adsorb gas, which is beneficial to shale gas enrichment. However, the $D2$ value should not be too large or too small. If $D2$ is too small, it indicates that the rock reservoir space is simple and mainly composed of macropores, and therefore, the adsorption capacity will not be high; if $D2$ is too large, it indicates that the rock pore structure is too complex and that the pore connectivity is extremely poor, resulting in difficulty in fracturing, exploitation, and mediocre economic efficiency. The shale of the Longmaxi Formation in the study area has large fractal dimensions ($D1$ and $D2$), indicating that there is a large proportion of micropores and mesopores in the reservoir space, with a small average pore size and a large specific surface area; this is conducive to the occurrence and storage of shale gas, especially adsorbed shale gas. However, due to the complex pore structure, poor connectivity, and small effective porosity, gas circulation is poor, and high requirements were imposed on the reservoir reconstruction measures during exploitation.

6.2. Influencing Factors of Pore Structure. It has been demonstrated that the development of shale pores is mainly

influenced by factors such as mineral composition, organic matter abundance, organic matter maturity, and diagenesis. In this study, correlation analysis was performed on the fractal dimension, organic matter abundance, and mineral composition (in this study, the organic matter maturity of shale samples from the Longmaxi Formation differed very little; therefore, the effect of maturity on the fractal dimension was excluded in the correlation analysis). The results show that the fractal dimension has a positive correlation with TOC (Figure 11), but $D1$ exhibits a weak increasing trend with the increase in TOC; this is because the shale samples in this study have high organic matter maturity and are in the overmature stage. In addition, it has been demonstrated that when the organic matter maturity is too high ($R_o > 3.0\%$) [32–34], organic matter is carbonized, some organic pores may collapse, and the adsorption capacity of organic matter will be greatly reduced so that the increase in the organic matter will not significantly improve the adsorption capacity of the shale. The fractal dimension is positively correlated with the content of clay minerals and pyrite but is negatively correlated with the content of quartz. This is because the clay minerals in the shale of the Longmaxi Formation in Laifeng, Hubei are mainly illite, which has a relatively weak adsorption capacity. As a result, the overall adsorption capacity of the clay minerals is low, and with the increased content, more intergranular pores and intergranular pores are developed, which improves the complexity of the pores. However, the improvement of the shale adsorption capacity is limited. Quartz is the main brittle mineral in rock and mainly develops intergranular pores with large pore sizes and simple structures. With the increasing content of quartz, the proportion of mesopores and macropores increases, the pore structure tends to be simple, and the adsorption and gas storage capacity of the shale decreases slightly. In addition, the presence of pyrite strongly indicates a reducing environment. The development of common organic matter between framboidal pyrite crystals is beneficial to the development and preservation of organic pores. Therefore, the fitting curve of the correlation between the fractal dimension and the pyrite content is consistent with that between the fractal dimension and the TOC.

7. Conclusion

(1) In well Ld1, the shale of the Longmaxi Formation is mainly siliceous shale, mixed shale, and clayey shale. Among them, the siliceous shale is mainly developed at the bottom and middle-upper part of the Longmaxi Formation; the mixed shale is mainly developed in the middle part, and; the clayey shale is mainly developed in the upper part. In the longitudinal direction, the mineral composition of the shale of the Longmaxi formation is highly heterogeneous; the amount of clay minerals gradually increases from bottom to top, and terrigenous detrital input also gradually increases from bottom to top. This indicates that the sea level gradually decreased from the early stage of the deposition of the Longmaxi Formation to the late stage and that the sedimentary environment gradually changed from a reducing environment to an oxidizing one. The siliceous shale (mostly high-carbon shale) at the bottom of the Longmaxi Formation has a high organic carbon content, and its microstructure is mostly blocky. The organic carbon content of the mixed shale and the clayey shale is relatively reduced as compared to the siliceous shale, and most are composed of low-carbon and carbon-poor shale, with obviously laminated microstructures. Furthermore, the occurrence, content, and brittleness of organic matter in the shales of different lithofacies are heterogeneous. Specifically, the siliceous shale at the bottom has the characteristics of high organic carbon content and good brittleness and is the key sweet interval in the study area

(2) According to the combined characterization and analysis based on mercury intrusion and low-temperature N_2 adsorption-desorption experiments, it is found that the pore structure of the shale in the Longmaxi Formation is complex and highly heterogeneous, with micropores and mesopores being the main pores and ink bottle pore being the main pore morphology. In addition, the fractal dimension of shale samples from the Longmaxi Formation was calculated based on the FHH equation; the results were as follows: $D1$ is 2.7284-2.7562 (mean: 2.7432) and $D2$ is 2.7984-2.8850 (mean: 2.8455), both of which are large. It is demonstrated by further analysis that the fractal dimension of pores can accurately represent the pore size, pore complexity, pore adsorption capacity, and gas storage capacity and can be used as a more comprehensive and effective characterization parameter of pore structure. The pore structure characteristics of the shale from the Longmaxi Formation in Laifeng, Hubei, are mainly as follows: a large proportion of micropores and mesopores are present in the reservoir space, the small average pore size is small, and the specific surface area is large, which is conducive to the occurrence and storage of shale gas, especially adsorbed shale gas; however, the complex pore structure, poor connectivity, and small effective porosity are not conducive to gas circulation. Therefore, higher requirements are required for reservoir reconstruction measures during exploitation

(3) The reservoir space of the shale from the Longmaxi Formation in Laifeng, Hubei, is mainly affected by organic matter abundance and mineral composition, and there is a positive correlation between the fractal dimension and the organic matter abundance. However, since most of the organic matter is in the overmature stage and has a reduced adsorption capacity, its controlling effect on the adsorption capacity of the shale is not obvious; the fractal dimension is positively correlated with the clay mineral and pyrite content but is negatively correlated with the quartz content

Data Availability

The data used to support the findings of this study are included within the article and are available from the corresponding author upon request.

Conflicts of Interest

The authors declare that they have no conflicts of interest.

Acknowledgments

This research was jointly supported by the Technical Fund Project of the Guizhou Science and Technology Department (QKHJC No. [2019]1293), Fund Project of the Department of Education of Guizhou Province (QJH No. KY [2018]029), Fund Program of the Science and Technology Department of Liupanshui City (52020-2018-03-03).

References

[1] R. G. Loucks, R. M. Reed, S. C. Ruppel, D. M. Jarvie, and D. M. Jarvie, "Morphology, genesis and distribution of nanometer-scale pores in siliceous mudstones of the Mississippian Barnett shale," *Journal of Sedimentary Research*, vol. 79, no. 12, pp. 848–861, 2009.

[2] J. Klaver, G. Desbois, G. Littke, and J. L. Urai, "BIB-SEM characterization of pore space morphology and distribution in postmature to overmature samples from the Haynesville and Bossier Shales," *Marine and Petroleum Geology*, vol. 59, pp. 451–466, 2015.

[3] R. G. Loucks, R. M. Reed, S. C. Ruppel, and U. Hammes, "Spectrum of pore types and networks in mudrocks and a descriptive classificanon for matrix-related mudrock pores-Spectrum of pore types and networks in mudrocks and a descriptive classification for matrix-related mudrock pores," *AAPG Bulletin*, vol. 96, no. 6, pp. 1071–1098, 2012.

[4] X. Z. Wang, L. X. Zhang, and C. Gao, "The heterogeneity of shale gas reservoir in the Yanchang formation, Xiasiwan area, Ordos Basin," *Earth Science Frontiers*, vol. 23, pp. 134–145, 2016.

[5] F. D. Zhao, Y. H. Guo, Y. M. Zhu, G. Wang, X. Chong, and X. M. Hu, "Analysis of microscale heterogeneity characteristics in marine shale gas reservoir: pore heterogeneity and its quantitative characterization," *Journal of China University of Mining and Technology*, vol. 17, pp. 296–307, 2018.

[6] Z. X. Zuo, X. B. Zhang, S. B. Chen, Q. H. Si, C. Zhang, and Z. Liu, "Heterogeneity of shale gas reservoirs in coal measures: a case study of the Taiyuan and Shanxi formations in the Ningwu Basin," *Acta Geologica Sinica*, vol. 91, pp. 1130–1140, 2017.

[7] X. B. Zhang, Z. Xi, C. Zuo, Q. H. Zhang, and Y. Z. Si, "Interlayer heterogeneity in pore structure of shale gas reservoir in the Yima area, Henan Province," *Acta Geoscientica Sinica*, vol. 37, pp. 340–348, 2016.

[8] C. Y. Lin, L. J. Tan, and C. L. Yu, "Research on the heterogeneous distribution of petroleum (I): original of the theory of hydrocarbon accumulation," *Lithologic Rcscrvoirs*, vol. 19, pp. 16–21, 2007.

[9] X. M. Xiao, Z. G. Song, Y. N. Zhu, H. Tian, and H. W. Yin, "Summary of shale gas research in north American and revelations to shale gas exploration of lower Paleozoic strata in China south area," *Journal of China Coal Society*, vol. 38, pp. 721–727, 2013.

[10] L. F. Lu, J. G. Cai, W. H. Liu, G. E. Teng, and J. Wan, "Occurrence and thermost ability of absorbed organic matter on clay minerals in mudstones and muddy sediments," *Oil & Gas Geology*, vol. 34, pp. 16–26, 2013.

[11] Y. Cai, D. Liu, Z. Pan, Y. Yao, J. Li, and Y. Qiu, "Pore structure and its impact on CH_4 adsorption capacity and flow capability of bituminous and subbituminous coals from Northeast China," *Fuel*, vol. 103, pp. 258–268, 2013.

[12] C. Liang, Z. X. Jiang, Y. C. Cao, M. H. Wu, L. Guo, and C. Zhang, "Deep-water depositional mechanisms and significance for unconventional hydrocarbon exploration: a case study from the lower Silurian Longmaxi shale in the southeastern Sichuan Basin," *AAPG Bulletin*, vol. 100, no. 5, pp. 773–794, 2016.

[13] C. Liang, Z. Jiang, Y. Yang, and X. Wei, "Shale lithofacies and reservoir space of the Wufeng-Longmaxi Formation, Sichuan Basin, China," *Petroleum Exploration and Development*, vol. 39, no. 6, pp. 736–743, 2012.

[14] F. Y. Wang, Z. Y. He, X. H. Meng, L. Y. Bao, and H. Zhang, "Occurrence of shale gas and prediction of original gas in-place (OGIP)," *Natural Gas Geoscience*, vol. 22, pp. 501–510, 2011.

[15] F. Yang, B. Y. Hu, S. Xu, Q. B. Meng, and B. M. Krooss, "Thermodynamic characteristic of methane sorption on shales from oil, gas, and condensate windows," *Energy & Fuels*, vol. 32, no. 10, pp. 10443–10456, 2018.

[16] B. Li, G. Q. Wei, K. Y. Hong, C. S. Peng, X. L. Hu, and L. L. Zhu, "Evaluation and understanding on the shale gas wells in complex tectonic provinces outside Sichuan Basin, South China: a case study from Well Laiye 1 in Laifeng-Xianfeng block, Hubei," *Natural Gas Industry*, vol. 36, pp. 29–35, 2016.

[17] Y. L. Zheng, C. L. Mu, Z. H. Xiao, X. P. Wang, X. L. Liu, and Y. Chen, "Characteristics and gas-bearing controlling factors of shale gas reservoir in complex tectonic provinces: a case from the lower Silurian Longmaxi formation of Well Laidi 1 in Laifeng-Xianfeng block, Hubei province," *Marine Origin Petroleum Gelogy*, vol. 25, pp. 108–120, 2020.

[18] J. Yu, J. Ma, J. G. Lu, Y. Cao, S. B. Feng, and W. C. Li, "Application of mercury injection and rate-controlled mercury penetration in quantitative characterization of microscopic pore structure of tight reservoirs: a case study of the Chang 7 reservoir in Huachi-Heshui area, the Ordos Basin," *Petroleum Geology & Experiment*, vol. 37, pp. 789–795, 2015.

[19] F. Yang, Z. F. Ning, Q. Wang, D. T. Kong, K. Peng, and L. F. Xiao, "Fractal characteristics of nanopore in shales," *Natural Gas Geoscience*, vol. 25, pp. 618–623, 2014.

[20] Z. D. Xi, S. H. Tang, J. Li, and L. Li, "Investigation of pore structure and fractal characteristics of marine-continental transitional shale in the east central of Qinshui Basin," *Natural Gas Geoscience*, vol. 28, pp. 366–376, 2017.

[21] P. Zhang, Y. Q. Huang, J. C. Zhang, H. Y. Liu, and J. W. Yang, "Fractal characteristics of the Longtan formation transitional shale in Northwest Guizhou," *Journal of China Coal Society*, vol. 43, pp. 1580–1588, 2018.

[22] J. H. Zhao, Z. J. Jin, Z. K. Jin et al., "Lithofacies types and sedimentary environment of shale in Wufeng-Longmaxi formation, Sichuan Basin," *Acta Petrolei Sinica*, vol. 37, pp. 572–586, 2016.

[23] Y. M. Wang, S. F. Wang, D. Z. Dong et al., "Lithofacies characterization of Longmaxi formation of the lower Silurian, southern Sichuan," *Earth Science Frontiers*, vol. 23, pp. 119–133, 2016.

[24] J. Z. Yi and C. Wang, "Differential pore development characteristics in various shale lithofacies of Longmaxi formation in Jiaoshiba area, Sichuan Basin," *Petroleum Geology & Experiment*, vol. 40, pp. 13–19, 2018.

[25] C. Zhong, Q. R. Qin, and J. L. Zhou, "Brittleness evaluation of organic-rich shale in Longmaxi formation in Dingshan area, southeastern Sichuan," *Geological Science and Technology Information*, vol. 379, pp. 167–174, 2018.

[26] Y. Hou, S. He, J. Yi et al., "Effect of pore structure on methane sorption potential of shales," *Petroleum Exploration and Development*, vol. 41, no. 2, pp. 272–281, 2014.

[27] H. Tian, S. C. Zhang, and S. B. Liu, "Determination of organic rich shale pore features by mercury injection and gas adsorption methods," *Acta Petrolei Sinica*, vol. 33, pp. 419–427, 2012.

[28] L. Hu, Y. M. Zhu, S. B. Chen, and Z. L. Du, "Fractal characteristics of shale pore structure of Longmaxi formation in Shuanghe area in southern Sichuan," *Xinjiang Petroleum Geology*, vol. 34, pp. 79–82, 2013.

[29] B. W. Du, X. H. Peng, S. K. Xie, and B. Zheng, "Exploration potential analysis of shale gas in the lower cretaceous, Gamba-Tingri basin of Tibet," *Petroleum Geology and Recovery Efficiency*, vol. 22, pp. 51–54, 2015.

[30] T. T. Cao, Z. G. Song, G. X. Liu, Q. Yin, and H. Y. Luo, "Characteristics of shale pores, fractal imension and their controlling factors determined by nitrogen dsorption and mercury injection methods," *Petroleum Geology and Recovery Efficiency*, vol. 23, pp. 1–8, 2016.

[31] Y. Gao, L. Mao, and R. Ma, "Pore structure characteristics and its fractal dimensions of transitional shales," *Science Technology and Engineering*, vol. 17, pp. 77–85, 2017.

[32] D. L. Xie, Y. H. Guo, and D. F. Zhao, "Fractal characteristics of adsorption pore of shale based on low temperature nitrogen experiment," *Journal of China Coal Society*, vol. 39, pp. 2466–2472, 2014.

[33] Y. M. Wang, D. Z. Dong, X. Z. Cheng, J. L. Huang, S. F. Wang, and S. Q. Wang, "Electric property evidences of the carbonification of organic matters in marine shales and its geologic significance: a case of the lower Cambrian Qiongzhusi shale in southern Sichuan Basin," *Natural Gas Industry*, vol. 34, pp. 1–7, 2014.

[34] F. Yang, Z. F. Ning, Q. Wang, and H. Q. Liu, "Pore structure of Cambrian shales from the Sichuan Basin in China and implications to gas storage," *Marine and Petroleum Geology*, vol. 70, pp. 14–26, 2016.